

Spin glass-like antiferromagnetic interactions in iron phosphate glasses

Joanna L. Shaw^a, Adrian C. Wright^{a,*}, Roger N. Sinclair^a, G. Kanishka Marasinghe^b, Diane Holland^c, Martin R. Lees^c, Charlie R. Scales^d

^a *J.J. Thomson Physical Laboratory, University of Reading, Whiteknights, Reading RG6 6AF, UK*

^b *Department of Physics, University of North Dakota, Grand Forks, ND 58202, USA*

^c *Department of Physics, University of Warwick, Coventry CV4 7AL, UK*

^d *BNFL, Building B170, Sellafield, Seascale, Cumbria CA13 1PG, UK*

Abstract

The phenomenon of spin freezing at low temperatures in iron-containing oxide glasses resulting from antiferromagnetic interactions has been previously reported for several oxide glass systems. The temperature dependence of the DC magnetic susceptibility has been measured with a SQUID magnetometer for a series of four iron oxide–phosphorus pentoxide glasses, containing between 30 and 44 mol% Fe₂O₃, and prepared so as to have an Fe³⁺ fraction of ~0.8. Well defined cusps are observed in the susceptibilities at temperatures between 5 K and 8 K for the four samples, cooled in zero field and measured at 0.025 T. As for classical metallic spin glass alloys, the susceptibilities measured after cooling from high temperature in this field are almost constant below the cusp temperatures, corresponding to spins freezing into a complicated configuration. Similar measurements at 0.5 T also demonstrate the freezing transition but the cusps in the susceptibility after zero-field cooling are broadened. The distribution and environments of iron ions within the samples are discussed in the light of the temperature-dependent magnetic structure factors and spin correlation functions, observed in neutron diffraction experiments on the same samples, along with the nuclear real space total correlation functions.

© 2004 Elsevier B.V. All rights reserved.

1. Introduction

Conventional spin glasses are magnetic materials in which there is some degree of long-range chemical and/or bond disorder, causing frustration at low temperatures of the antiferromagnetic spin interactions of nearest neighbors. An indication of the magnetic character of a material can be obtained from measurements of the linear magnetic susceptibility, χ , as a function of temperature, T , according to the Curie–Weiss equation [1],

$$\chi = \frac{M}{H} = \frac{C}{T - \theta_p}, \quad (1)$$

where M is the magnetization, at a given field, H , C is the Curie constant, and θ_p is the paramagnetic temperature. A negative value of θ_p indicates antiferromagnetic interactions, while a positive value implies ferromagnetic. Hence a negative paramagnetic temperature should be displayed for a spin glass-like system.

Spin glass behavior is further characterized by a cusp in the linear magnetic susceptibility measured against temperature (e.g. see Fig. 1), first found for gold–iron alloys by Canella and Mydosh in 1972 [2]. Cooling the sample below the cusp temperature in an applied magnetic field will freeze the spins into their frustrated state

* Corresponding author. Tel.: +44 118 378 8555; fax: +44 118 975 0203.

E-mail address: a.c.wright@rdg.ac.uk (A.C. Wright).

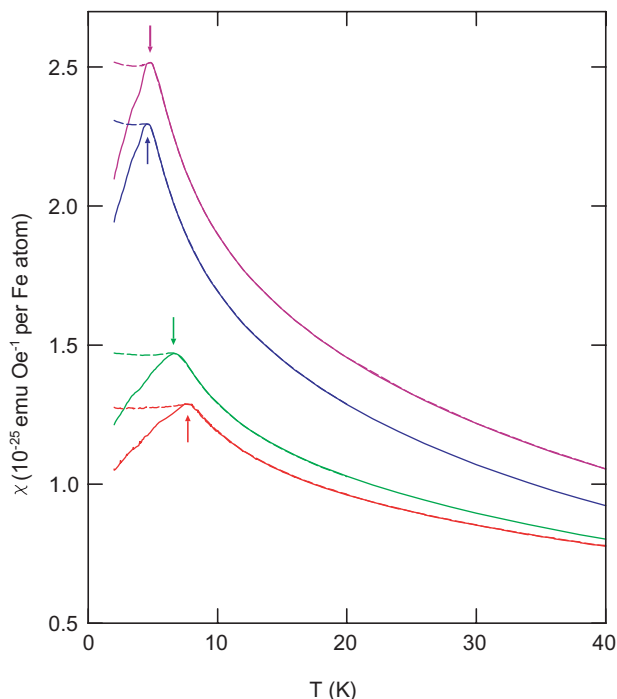


Fig. 1. Linear magnetic susceptibilities for the field (---) and zero-field (—) cooled 30Fe70P (magenta), 35Fe65P (blue), 40Fe60P (green) and 44Fe56P (red) iron phosphate glasses measured at a field of 0.025 T. The arrows indicate the spin freezing transition temperatures, T_f . (For interpretation of the references in colour in this figure legend, the reader is referred to the web version of this article).

and leave an almost temperature-independent magnetization. With zero-field cooling, the spins can relax and the susceptibility reduces with temperature. Thus it is apparent that some transition occurs at the cusp temperature (hereafter referred to as T_f , the spin freezing temperature). This transition has been widely studied [3–7], although its nature is still not clear.

Studies of early spin glass systems looked at dilute crystalline alloys of transition metals in noble metal hosts, but the term has now come to encompass a much wider range of materials, including more magnetically concentrated insulators, and amorphous systems. Various iron-containing oxide glasses display the phenomenon of spin freezing at low temperatures, for instance sodium germanates and sodium silicates [8], aluminosilicates [5,9,10], and phosphates [11,12].

Iron phosphate glasses are of increasing interest not only magnetically, but electrically, structurally and chemically as well [13–23]. They are known to exhibit semiconducting properties, since iron exists in the glass in the two valence states, Fe^{2+} and Fe^{3+} [15,24]. In addition, they have high chemical durability as compared to other phosphate glasses, making them a prime candidate for vitrifying nuclear wastes, particularly those containing plutonium, [13,14,21–23,25] and also for such applications as biomedical components and glass-to-metal seals [20]. Normally, phosphate glasses are vulnerable

to hydration via the P–O–P linkage, where O represents a bridging oxygen atom, but it is thought that the formation of the more resistant Fe–O–P linkage in iron phosphate glasses is responsible for the greater resilience of these materials [16,20].

Fe_2O_3 – P_2O_5 glasses with high Fe_2O_3 content are particularly interesting, in that they exhibit short-range antiferromagnetic (speromagnetic) ordering at low temperatures [26,27], which decays with increasing temperature. This was revealed by an early neutron magnetic scattering study of a glass of composition $0.79\text{Fe}_2\text{O}_3 \cdot \text{P}_2\text{O}_5$ (44 mol% Fe_2O_3), which involved measuring the diffraction pattern above (77 K) and below (4 K) the magnetic short-range ordering transition [27]. The data were Fourier transformed to yield the real space magnetic correlation function, $D^M(r)$, the first real peak of which is negative, thus indicating the antiferromagnetic nature of the short-range magnetic ordering (i.e. speromagnetism). The peaks in $D^M(r)$ also give the Fe–Fe distances in the glass, which are found to be very similar to those in α -quartz FePO_4 .

Crystalline FePO_4 ($\text{Fe}_2\text{O}_3 \cdot \text{P}_2\text{O}_5$) is a structural analogue of SiO_2 and exhibits both α - and β -quartz polymorphs, with alternate corner sharing FeO_4 and PO_4 tetrahedral structural units [28]. (Note that the requirement for alternating tetrahedra means the various III–V and II–VI analogues of SiO_2 are limited to those polymorphs which contain only even-membered rings.) Although Fe_2O_3 – P_2O_5 glasses are formed with excess P_2O_5 , they are not formed at the 1:1 stoichiometry and this has been used as an argument that odd-membered rings must be present in vitreous silica and related tetrahedral random network glasses [28]. (Note also that there is controversy in the literature concerning the glass-forming region for the Fe_2O_3 – P_2O_5 system, due to the fact that the glasses contain a variable amount of Fe^{2+} , depending on the preparation conditions [29].)

A possible structural model for Fe_2O_3 – P_2O_5 glasses with excess P_2O_5 , based on the α - and β -quartz polymorphs of FePO_4 , involves three structural units—alternating FeO_4 and PO_4 tetrahedra sharing all four corners and $\text{O}=\text{P}\text{O}_3$ units (i.e. PO_4 tetrahedra with one terminal double-bonded oxygen and three corner sharing single-bonded oxygen atoms), which can be incorporated into odd membered rings [27], and hence allow frustrated interaction around the rings. However, this might lead to the micro-separation of an α - FePO_4 -containing phase. An alternative structural model, for glasses containing significant concentrations of Fe^{2+} , has been proposed by Marasinghe et al. [29], based on the crystal structure of $\text{Fe}_3(\text{P}_2\text{O}_7)_2$ in which the iron is present as $(\text{Fe}_3\text{O}_{12})^{16-}$ clusters comprising one Fe^{2+} and two Fe^{3+} ions, all in six-fold co-ordination.

The present paper reports magnetic susceptibility data for four glasses in the iron phosphate system, of nominal composition $x\text{Fe}_2\text{O}_3 \cdot (1-x)\text{P}_2\text{O}_5$ ($x = 0.30$,

0.35, 0.40, 0.44). However, as indicated above, they are in fact oxygen deficient due to the reduction of some of the iron to Fe^{2+} , despite being prepared in such a way as to maximize the Fe^{3+} content {to a value of ~ 0.8 for the ratio $\text{Fe}^{3+}/(\text{Fe}^{2+} + \text{Fe}^{3+})$ [16,29]}. The notation used here for the respective glasses will be 30Fe70P, 35Fe65P, 40Fe60P and 44Fe56P. The data collected yield information on the environments of iron ions within the samples, and on the resulting magnetic nature of the glasses. Both nuclear and magnetic neutron diffraction techniques have also been employed to investigate these samples [30], but the results will be reported elsewhere due to space limitations.

2. Experimental details

Four glasses of composition $x\text{Fe}_2\text{O}_3 \cdot (1-x)\text{P}_2\text{O}_5$ $\{x = 0.30, 0.35, 0.40, 0.44\}$ were prepared at the University of Missouri–Rolla, USA, by melting in an atmosphere of air at 1150°C for 1–2 h in alumina crucibles. Full details of the sample preparation and characterization have been published elsewhere [16,29]. The preparation conditions were set so as to obtain an Fe^{3+} fraction of ~ 0.8 in the glasses. (Exact values of the iron ion ratios will be determined using Mössbauer techniques and reported at a future time.) After heating, the samples were quenched by pouring onto stainless steel plates, annealed for ~ 3 h at 450°C , and powdered for experiment. The powders were checked for crystalline phases using X-ray diffraction. The bulk sample densities were measured with a Quantachrome Micropycnometer at the Rutherford Appleton Laboratory (Chilton, UK) and are given in Table 1.

Measurements of the dc susceptibility as a function of temperature were taken for each composition in a field of 0.025 T (250 G) and additionally for the 30Fe70P and 44Fe56P compositions in a high field of 0.5 T (5000 G) using a SQUID magnetometer at the University of Warwick. The temperature range employed was 2–150 K. The data were collected after cooling to 2 K both in a magnetic field and in zero field to observe the magnetization behavior. The dependence of the sample magnetization upon applied field was also investi-

gated by performing sweeps over a field of zero to 5 T at constant temperature, for a range of temperatures (5, 20, 50, 100, 200 and 300 K). The susceptibilities were calculated as susceptibilities per iron atom by dividing by the number of iron atoms in the mass of sample used for the measurements.

3. Results

Graphs of the low field (0.025 T) DC magnetic susceptibilities per iron atom are presented for each sample in Fig. 1, including both the field cooled and the zero-field cooled behavior. The positions of the spin freezing transition temperatures, T_f , are indicated by the arrows. Measurements taken at 0.5 T give similar results, but the cusps in the susceptibilities after zero-field cooling are broadened due to saturation of the spins. The values of T_f , together with the peak susceptibilities, χ_{peak} , the Curie constants, C , and the paramagnetic temperatures, θ_p , are given in Table 1. These latter two were deduced from the gradient and intercept, respectively, of a linear fit to the high temperature region of the susceptibility data, according to Eq. (1), by plotting χ^{-1} against T . Also included in the table are the temperatures of the

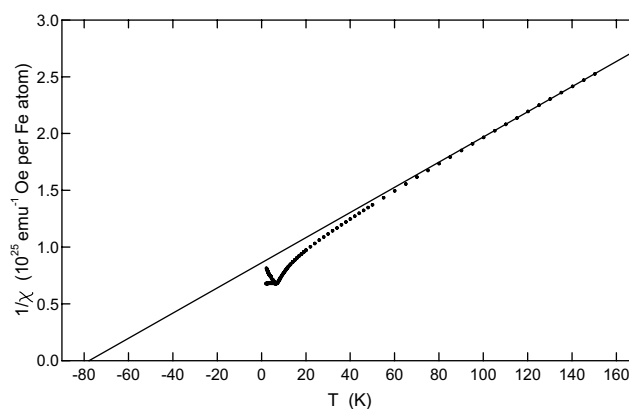


Fig. 2. Fit of the Curie–Weiss law above 110 K (—) to the experimental magnetic susceptibility data (●) for the 40Fe60P iron phosphate glass. The gradient gives the Curie constant, C , and the intercept gives the paramagnetic temperature, θ_p .

Table 1
Sample densities and magnetic susceptibility parameters for iron phosphate glasses

Field (T)	Sample	Density (gcm^{-3})	T_f (K)	χ_{peak} ($10^{-25} \text{emu Oe}^{-1}$)	T_{onset} (K)	C ($10^{-25} \text{emu K Oe}^{-1}$)	θ_p (K)	p
0.025	30Fe70P	2.967 ± 0.003	4.79 ± 0.10	2.52 ± 0.05	65 ± 5	8.25 ± 0.03	-39.2 ± 1.0	6.3 ± 0.2
0.025	35Fe65P	2.945 ± 0.003	4.59 ± 0.10	2.31 ± 0.05	55 ± 5	6.97 ± 0.02	-36.6 ± 0.5	5.8 ± 0.4
0.025	40Fe60P	3.039 ± 0.003	6.59 ± 0.20	1.47 ± 0.05	115 ± 5	9.03 ± 0.08	-77.8 ± 1.9	6.6 ± 0.3
0.025	44Fe56P	3.086 ± 0.003	7.69 ± 0.30	1.29 ± 0.05	135 ± 10	13.4 ± 0.4	-149 ± 9	8.0 ± 0.6
0.5	30Fe70P	2.967 ± 0.003	3.09 ± 0.10	2.35 ± 0.05	85 ± 5	8.20 ± 0.09	-38 ± 2	6.8 ± 0.3
0.5	44Fe56P	3.086 ± 0.003	5.69 ± 0.80	1.14 ± 0.05	115 ± 10	8.13 ± 0.11	-85 ± 2	6.3 ± 0.3

The peak susceptibilities, χ_{peak} , Curie constant, C , and effective magneton number, p , are given per iron atom.

onset of Curie–Weiss behavior; i.e. above these temperatures the glasses behave according to Eq. (1), and below the experimental data deviate from the fit and spin glass-like interactions dominate in the system. An example of such a fit is shown in Fig. 2 for the 40Fe60P data. Effective magneton numbers, p , (Table 1) were derived, for each sample and for the two field strengths used in the susceptibility measurements, from the Curie constant [1],

$$C = p^2 \mu_B^2 / 3k_B, \quad (2)$$

μ_B being the Bohr magneton and k_B the Boltzmann constant.

4. Discussion

The four samples display behavior typical of spin glass systems, namely the cusps in the low temperature susceptibility data and the negative values of the paramagnetic temperatures which indicate antiferromagnetic interactions between the spins. A well-defined cusp in the temperature dependence of the linear magnetic susceptibility, χ_m , is displayed for all compositions when measured in a field of 0.025 T (250 G). (cf. Figs. 1 and 2). Similar results were found for the two samples measured at the higher field of 0.5 T (5000 G), but the cusps are broadened. It is clear that in this case the field was too high to allow a proper investigation of the cusp temperature, since saturation was approached and the interesting features were broadened.

The effective magneton number, p , derived for each sample from the application of the simple Curie–Weiss model of paramagnetic behavior [1] at higher temperatures (Table 1), may be compared to the published values for iron group salts [1]. The average experimental value for Fe^{3+} ions of 5.9 is closer to the measured values than the average value of 5.4 for Fe^{2+} ions. This indicates that, as expected from the chosen preparation conditions, the concentration of Fe^{3+} ions is much greater than that of Fe^{2+} ions.

Low-field measurements taken after cooling the sample to 2 K in zero field gave cusp (spin-freezing) temperatures, T_f , between 4 K and 8 K, as listed in Table 1 together with the peak susceptibility for each composition. The positions of T_f are indicated in Fig. 1 by arrows. The parameters in Table 1 are all of the same order of magnitude compared with other amorphous spin glass-like systems [5,8–12]. The difference in the field-cooled and zero-field cooled susceptibilities (Fig. 1) shows that, as for the classical metallic spin glass alloys, the susceptibilities measured after cooling from high temperature with the field applied are almost constant below T_f , corresponding to spins freezing into a complicated configuration. Zero-field cooling allows a relaxation of the spins below the critical temperature.

An interesting feature of the susceptibilities at higher temperature, for the different samples, is the cross-over in their values, beginning at $T \sim 55$ K. As the temperature is increased from this point, the susceptibility for the 44 mol% sample crosses the others in turn to become the highest in value by the time it reaches 150 K. The 40 mol% line also swaps position with the 35 mol% so that they then decrease in the order 44, 30, 40, 35 mol% Fe_2O_3 at 150 K. However, were the data taken to higher temperatures, the lines would continue crossing each other as the temperature rises further and the magnitudes of χ would then be in order of decreasing iron content. Since χ is, of course, a quantity dependent on the magnetization of a material, i.e. its ability to become magnetized, it is logical that at temperatures where the thermal agitation is too great to allow the speromagnetic ordering, the material with the largest concentration of a magnetic species would have the greatest susceptibility. The higher concentration of magnetic species means there are a greater number of the iron clusters and/or that they are greater in size. Either way, the distance between them is reduced and at low temperatures the spin correlations are more easily transmitted, so enabling the system to exist in a higher degree of order. The neutron magnetic scattering revealed the speromagnetic characteristics of the glasses, and hence it is to be expected that an ordering of the spins results in their *cancellation* due to the antiparallel arrangement. The suggestion is therefore that, with increasing iron content, the speromagnetic spin interactions become more antiferromagnetic in nature (increasing θ_p , cf. Table 1) and accordingly result in a lower level of magnetization and susceptibility of the material. These results support the conclusions of the neutron scattering experiments [30].

The susceptibility taken as a function of temperature can be re-plotted as T against $1/\chi_m$. It is possible to fit a straight line to the high temperature region of the graph where the sample behaves paramagnetically. If the material were truly paramagnetic at all temperatures, the straight line would pass through the origin and have a gradient of C , the Curie constant, according to the Curie law. In practice, however, the line has a negative ordinate intercept equal to the paramagnetic temperature, θ_p cf. Eq. (1). One of the graphs plotted in this way is shown in Fig. 2, and the values obtained for θ_p and C are listed in Table 1, as well as the temperature at which the curve deviates from the fitted straight line and therefore no longer behaves paramagnetically.

An alternative path to finding values for these parameters is to consider the measurements taken at constant temperatures while the magnitude of the applied field was varied. A simple plot of MT against H results in a series of (almost) straight lines emanating from the origin with different positive gradients.

By subtracting a constant from the measurement temperature, the lines can be scaled on top of one another. The graphs are then essentially plots of the Curie–Weiss law once more ($M(T - \theta_p)$ plotted against H), and the temperature constant is the paramagnetic temperature, θ_p . The gradient of the scaled lines is simply the Curie constant, C . Curie–Weiss plots were generated in this way for each sample.

Agreement between θ_p and C , obtained by these methods, is not within the errors but is at least reasonable for the two lowest iron compositions. The reason is almost definitely that the errors given in the table for the straight line fitting do not accurately reflect the real uncertainty, since a small degree of curvature remains for the high-iron susceptibility data even at the largest temperature considered.

For many of the magnetic parameters in Table 1, the values for the 35Fe65P sample are slightly lower than those of the 30Fe70P sample, but rise again for the two highest iron content glasses. An example of this trend is shown for the density in Fig. 3. These results are puzzling, especially as the phenomenon is not seen in the peak susceptibility values, χ_{peak} . There is an uneven spacing of the susceptibilities of Fig. 1 with a gap between 35 mol% and 40 mol% that cannot be attributed to iron content, but they at least remain in order of iron concentration. The reason for this gap is also not yet understood, and it is possible that it is related to the anomaly in the parameters. A potential explanation for the anomaly may lie with the $\text{Fe}^{3+}/(\text{Fe}^{2+} + \text{Fe}^{3+})$ ratio. Magnetically, Fe^{3+} ions may have a greater influence than Fe^{2+} ions since the spherically symmetric electron distribution allows for an easier alignment of Fe^{3+} . Therefore if some of the samples contain concentrations of Fe^{3+} that were not expected from the preparation conditions, it should be apparent in the magnetic parameters. Hence a reduced Fe^{3+} content in the 35Fe65P glass relative to the other samples

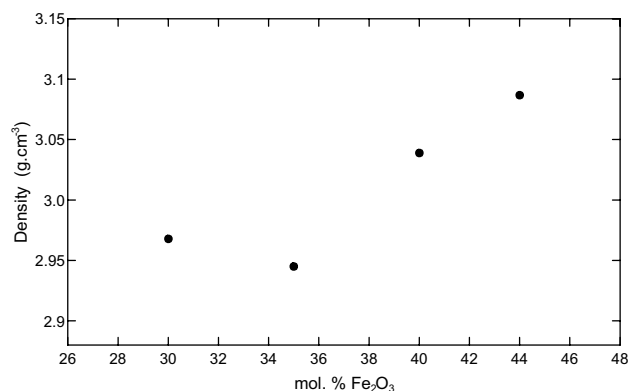


Fig. 3. Densities of the four iron phosphate glasses, showing the dip in value for the 35Fe65P sample relative to the others, typical of the parameters in Table 1. The error bars are within the point symbols.

would also lessen the magnetic characteristics, and, in addition, cause a decrease in the sample density, since the co-ordination of Fe^{2+} ions is higher than for Fe^{3+} . However, only a reasonably large difference in the Fe^{2+} content of the samples could explain the density disparity seen with these samples if this is indeed its cause. Alternatively, it may be that the 35Fe65P composition is close to some structure which results in a less compact atomic arrangement within the glass. The gap seen in the susceptibility data of Fig. 1 between the 35Fe65P and 40Fe60P samples is probably related to this parameter anomaly also. It is hoped that, together with neutron data for the systems, Mössbauer analysis of the iron ion ratios will help to clarify this matter.

5. Conclusions

The magnetic nature of four iron phosphate glasses was investigated using a SQUID magnetometer to measure the DC susceptibilities for a low field (0.025 T) and 0.5 T. Below the region between 65 and 135 K, the glasses all exhibit spin glass-like antiferromagnetic interactions, demonstrated by the characteristic cusps in the susceptibilities and the negative values of the paramagnetic temperatures, θ_p . The cusp temperatures, T_f , have been identified as spin freezing temperatures, with values between 5 K and 8 K. When the samples were cooled in an applied field, the susceptibility remained nearly constant below T_f , but decreased with temperature for zero-field cooled measurements. Values of the Curie constant (C), paramagnetic temperatures (θ_p) and effective magneton number (p) were found for each sample. However, the use of Eq. (1) could only yield indicative values, since the data were not taken to high enough temperatures for the susceptibility to become linear. Hence the attempt of fitting a straight line to curved data introduced systematic errors. All of the θ_p values were negative and, in general, the antiferromagnetic interaction strengthened with increasing iron content. The derived effective magneton numbers indicated that Fe^{3+} is the dominant iron species, as expected. The Fe^{3+} to Fe^{2+} ratio will be measured by Mössbauer spectroscopy and will be used to further interpret the present data, together with those obtained by neutron scattering.

Acknowledgment

The authors would like to thank Alex Hannon at the Rutherford Appleton Laboratory for his help and the use of the Quantachrome Micropycnometer. J.L.S. would like to thank BNFL for a PhD studentship.

References

- [1] C. Kittel, Introduction to Solid State Physics, 7th Ed., Wiley, New York, 1996, Chap. 14 & 15.
- [2] V. Cannella, J.A. Mydosh, Phys. Rev. B 6 (1972) 4220.
- [3] S.F. Edwards, P.W. Anderson, J. Phys. F 5 (1975) 965.
- [4] M.J.P. Gingras, C.V. Stager, N.P. Raju, B.D. Gaulin, J.E. Greedan, Phys. Rev. Lett. 78 (1997) 947.
- [5] J.P. Sanchez, J.M. Friedt, R. Horne, A.J. van Duynveldt, J. Phys. C 17 (1984) 127.
- [6] J.K. Warner, A.K. Cheetham, A.G. Nord, R.B. Von Dreele, M. Yethiras, J. Mater. Chem. 2 (1992) 191.
- [7] J.S. Gardner, B.D. Gaulin, S.-H. Lee, C. Broholm, N.P. Raju, J.E. Greedan, Phys. Rev. Lett. 83 (1999) 211.
- [8] Kh.A. Ziq, A. Mekki, J. Non-Cryst. Solids 293–295 (2001) 688.
- [9] W. Nägele, K. Knorr, W. Prandl, P. Convert, J.L. Buevoz, J. Phys. C 11 (1978) 3295.
- [10] J. Ferré, J. Pommier, J.P. Renard, K. Knorr, J. Phys. C 13 (1980) 3697.
- [11] T. Egami, O.A. Sacli, A.W. Simpson, A.L. Terry, F.A. Wedgwood, J. Phys. C 5 (1972) L261.
- [12] G.J. Long, A.K. Cheetham, P.D. Battle, Inorg. Chem. 22 (1983) 3012.
- [13] G.K. Marasinghe, M. Karabulut, C.S. Ray, D.E. Day, D.K. Shuh, P.G. Allen, M.-L. Saboungi, M. Grimsditch, D. Haefner, J. Non-Cryst. Solids 263 (2000) 146.
- [14] M. Karabulut, G.K. Marasinghe, C.S. Ray, G.D. Waddill, D.E. Day, Y.S. Badyal, M.-L. Saboungi, S. Shastri, D. Haefner, J. Appl. Phys. 87 (2000) 2185.
- [15] A. Mogus-Milankovic, D.E. Day, J. Non-Cryst. Solids 162 (1993) 275.
- [16] X. Fang, C.S. Ray, A. Mogus-Milankovic, D.E. Day, J. Non-Cryst. Solids 283 (2001) 162.
- [17] M. Chybicki, J. Nowatowski, W. Sadowski, Phys. Stat. Sol. (a) 68 (1981) K129.
- [18] T. Tsuchiya, M. Otonari, T. Ariyama, Nippon Seram Kyo Gak 95 (1987) 295.
- [19] T. Tsuchiya, N. Yoshimura, J. Mater. Sci. 24 (1989) 493.
- [20] T. Jermoumi, M. Hafid, N. Toreis, Phys. Chem. Glasses 43 (2002) 129.
- [21] S.T. Reis, M. Karabulut, D.E. Day, J. Nucl. Mater. 304 (2002) 87.
- [22] S.T. Reis, D.L.A. Faria, J.R. Martinelli, N.M. Pontuschka, D.E. Day, C.M. Partiti, J. Non-Cryst. Solids 304 (2002) 188.
- [23] C.S. Ray, X. Fang, M. Karabulut, G.K. Marasinghe, D.E. Day, J. Non-Cryst. Solids 249 (1999) 1.
- [24] E.J. Friebele, L.K. Wilson, A.W. Dozier, D.L. Kinser, Phys. Stat. Sol. (b) 45 (1971) 323.
- [25] M. Karabulut, G.K. Marasinghe, C.S. Ray, D.E. Day, G.D. Waddill, C.H. Booth, J.J. Butcher, D.L. Caulder, D.K. Shuh, P.G. Allen, M. Grimsditch, J. Mater. Res. 15 (2000) 1972.
- [26] T. Egami, O.A. Sacli, A.W. Simpson, A.L. Terry, in: H.O. Hooper, A.M. deGraaf (Eds.), Amorphous Magnetism, Plenum, New York, 1973, p. 27.
- [27] F.A. Wedgwood, A.C. Wright, J. Non-Cryst. Solids 21 (1976) 95.
- [28] A.C. Wright, J.A.E. Desa, Phys. Chem. Glasses 19 (1978) 140.
- [29] G.K. Marasinghe, M. Karabulut, C.S. Ray, D.E. Day, M.G. Shurnsky, W.B. Yelon, C.H. Booth, P.G. Allen, D.K. Shuh, J. Non-Cryst. Solids 222 (1997) 144.
- [30] J.L. Shaw, PhD thesis, University of Reading, 2003.